16

Barton, C. A., and M. D. Zoback, 2002, Wellbore imaging technologies applied to reservoir geomechanics and environmental engineering, *in* M. Lovell and N. Parkinson, eds., Geological applications of well logs: AAPG Methods in Exploration, No. 13, p. 229–239.

Wellbore Imaging Technologies Applied to Reservoir Geomechanics and Environmental Engineering

Colleen A. Barton
GeoMechanics International, Inc.
Palo Alto, California, U.S.A.

Mark D. Zoback
Stanford University
Department of Geophysics
Stanford, California, U.S.A.

ABSTRACT

Drilling-induced wellbore failures provide critical constraints on the in-situ state of stress. Knowledge of the relationship between natural fracture systems and tectonic stresses has direct application to problems of reservoir performance, fluid migration, and wellbore stability. Acoustic, electrical, and optical wellbore images provide the means to detect and characterize natural fracture systems and to discriminate these from induced wellbore failures. New techniques of wellbore-image analysis are presented to distinguish attributes of natural fractures from induced failures in borehole-image data. The performance of low-permeability fractured reservoirs is controlled by the in-situ state of stress and by the distribution and orientation of natural fractures and faults. We discuss case studies of the relationships among natural fracture systems, in-situ stress, and permeability. These case studies involve geothermal reservoirs and a petroleum reservoir; one case study involves geotechnical site characterization.

INTRODUCTION

Wellbore-image logs are extremely useful for identification and study of modes of stress-induced wellbore failures. We present examples that show how these wellbore failures appear in different types of image data and how they can be discriminated from natural fractures that are intersected by the wellbore. Then we present brief overviews of studies that illustrate how the techniques of discrimination have been applied to address specific issues of fracture permeability.

Drilling-induced failures are extremely common in oil wells, gas wells, and geothermal wells because the drilling of a well causes concentration of the far-field tectonic stress close to the wellbore; this stress commonly exceeds strength of the rock. Through use of wellbore imaging and other logging techniques, stress-induced failures can be detected and classified (compressive, tensile, or shear) and then used to estimate the unknown components of the stress field. We demonstrate how these modes of wellbore failure appear in different types of image data and the pitfalls in the interpretation of failures.

The most valuable use of drilling-induced features is to constrain the orientations and magnitudes of the current natural stress field. Use of drilling-induced features as stress indicators has become routine in the petroleum industry

(Peska and Zoback, 1995; Zoback and Peska, 1995; Willson et al., 1999; Brudy and Kjorholt, 1999; Stjern et al., 2000; Castillo and Moos, 2000; Wiprut and Zoback, 2000; Brudy and Zoback, 1999; and numerous other authors). Detection of these features at the wellbore wall has become a primary target for LWD/MWD (logging while drilling/measurement while drilling) real-time operations (Rezmer-Cooper et al., 2000).

Strong correlation between critically stressed fractures (fractures optimally oriented to the stress field for frictional failure) and hydraulic conductivity has been documented in a variety of reservoirs worldwide (Barton et al., 1995; Barton et al., 1998). When faults are critically stressed, permeabilities are increased and the movement of fluid along faults is possible. We present examples of how knowledge of the stress state and natural fracture population can be used to access reservoir permeability.

In environmental and geotechnical applications, the identification and prediction of permeable fracture systems—along which contaminants or groundwater could flow—are primary purposes of most site-characterization studies. We demonstrate how the technologies we have developed to analyze and characterize fracture systems and to determine the state of in-situ stress can be applied directly to management of shallow, fractured aquifers as well as to deep reservoirs.

DRILLING-INDUCED FAILURE OF BOREHOLE WALLS

Compressive and tensile failure of a wellbore are direct results of stress concentration around a wellbore; the concentration results from drilling a well into an already stressed rock mass (Moos and Zoback, 1990). Compressive wellbore failures (wellbore breakouts), first identified from caliper data, are useful for determination of stress orientation in vertical wells (Gough and Bell, 1981; Zoback et al., 1985; Plumb and Hickman, 1985). Study of such features with acoustic and electrical imaging devices makes it possible to identify such features clearly and to use them for stress-magnitude determination as well as stress orientation (Zoback et al., 1985; Barton et al., 1988; Shamir and Zoback, 1992; Barton et al., 1997).

If a wellbore is pressurized to a critical level, a hydraulic fracture forms at the azimuth of the maximum horizontal stress (Hubbert and Willis, 1957). Formation of drilling-induced tensile wall fractures is the result of the natural stress state, perhaps aided by drilling-related perturbations. The natural state of stress causes the wellbore wall to fail in tension.

The general case of tensile and compressive failure of arbitrarily inclined wellbores in different stress fields is described by Peska and Zoback (1995). They demonstrated that there is a wide range of stress conditions under which drilling-induced tensile fractures occur in wellbores, even without significant wellbore-fluid overpressure. We call these fractures "tensile wall fractures," because they develop only in the wellbore wall, as a result of concentration of stress. In vertical boreholes (Figure 1a), these failures form in the orientation of the maximum principal horizontal stress. In deviated wells (Figure 1b), they form as en-echelon features. Because drilling-induced tensile wall fractures are very sensitive to in-situ stress, they can be used for constraining the present state of stress (Hayashi and Abe, 1984; Aadnoy, 1990; Brudy and Zoback, 1993; Okabe et al., 1996; Peska and Zoback, 1995; Zoback and Peska, 1995).

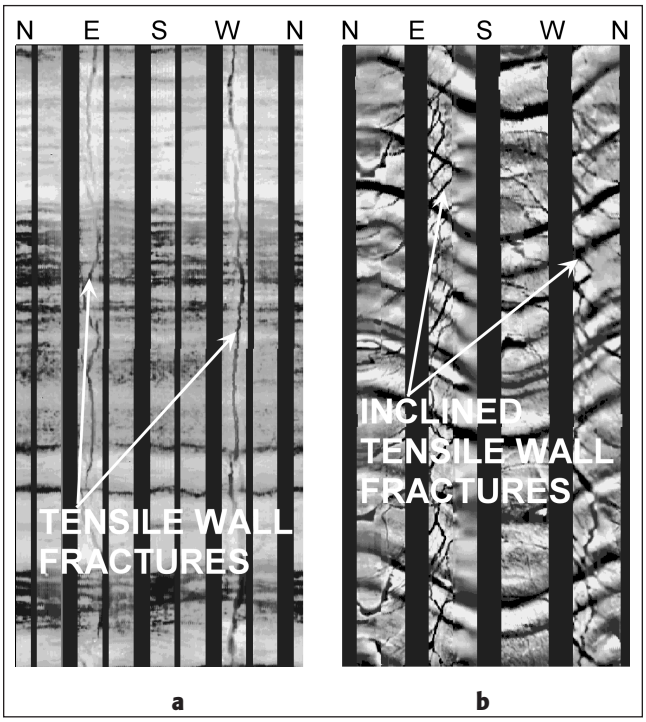

Figure 1. Electrical-image data showing (a) typical drilling-induced tensile wall fractures in a vertical borehole and (b) inclined tensile fractures in a deviated borehole.

PITFALLS IN INTERPRETATION OF TENSILE WALL FRACTURES IN WELLBORE-IMAGE DATA

In cases in which drilling-induced tensile fractures form at angles to the wellbore axis, it can be difficult to distinguish them from natural fractures (especially in electrical-image logs that do not sample the entire wellbore circumference). Misinterpretation of such features could lead to serious errors in characterization of a fractured (or perhaps not fractured!) reservoir, as well as in the assessment of in-situ stress orientation and magnitude. Therefore, we present criteria that are

useful for discriminating natural fractures from induced tensile fractures, when such features are observed in wellbore-image logs.

This is especially important because wellbore-stress concentration can have significant effect on the appearances of natural fractures that intersect the wellbore. Fractures are weakened mechanically at intersections with the borehole. In the standard 2-D unwrapped view of wellbore-image data this erosion causes the upper and lower "peak" and "trough" of the fracture sinusoid to be enlarged and then enhanced (Figure 2).

Where borehole-hoop stress is tensile, the intersection of a natural fracture or foliation plane with the tensile region of the borehole may be opened preferentially in tension (Figure 3a). These drilling-enhanced natural fractures can be mistaken easily for inclined tensile wellbore failures (Figure 1b), resulting in serious errors in geomechanical modeling.

Incipient wellbore breakouts develop where concentration of borehole compressive stress exceeds the rock's strength. However, the failed material within the breakout has not spalled into the borehole (Figure 3b). In a vertical borehole, these failures may be shown as thin "fractures" that have propagated vertically; they may be confused with drilling-induced tensile wall cracks.

Where image data are ambiguous and misinterpretation is probable to a significant degree, strict criteria are needed for reliable interpretation of images. In many instances, both drilling-induced and drilling-enhanced fractures form a systematic set with features that are similar over a range of depths—for example, in en-echelon fashion (Figures 1b and 3a). One of the best methods for discrimination between inclined drilling-induced fractures and drilling-enhanced natural fractures is to attempt to fit a flexible sinusoid to the "pair" of features. Because drilling-induced tensile wall fractures are discontinuous around the wellbore circumference (they can propagate only in the tensile region of the borehole), they cannot be fitted to a sinusoidal shape. In contrast, drilling-enhanced natural fractures can be fitted by a flexible sinusoid.

For accurate measurement of the azimuth and inclination of true induced tensile wall fractures, the most effective approach is to use a specially designed interactive image-analysis tool, which can be used to fit the orientations and lengths of fractures.

When interpreting possible incipient wellbore breakouts, understanding the wellbore stress state is also essential. Incipient breakouts should form in sets of four fine-scale vertical features, unlike induced tensile wall fractures, which form only two diametrically opposite fractures. Where wellbore breakouts are in data under investigation, incipient breakouts should be at azimuths consistent with the outer edges of well-developed breakouts within the compressional region of the borehole (Figure 4a). The best way to analyze wellbore breakouts and incipient wellbore breakouts is by use of polar cross sections of acoustic wellbore-image data (Figure 4b).

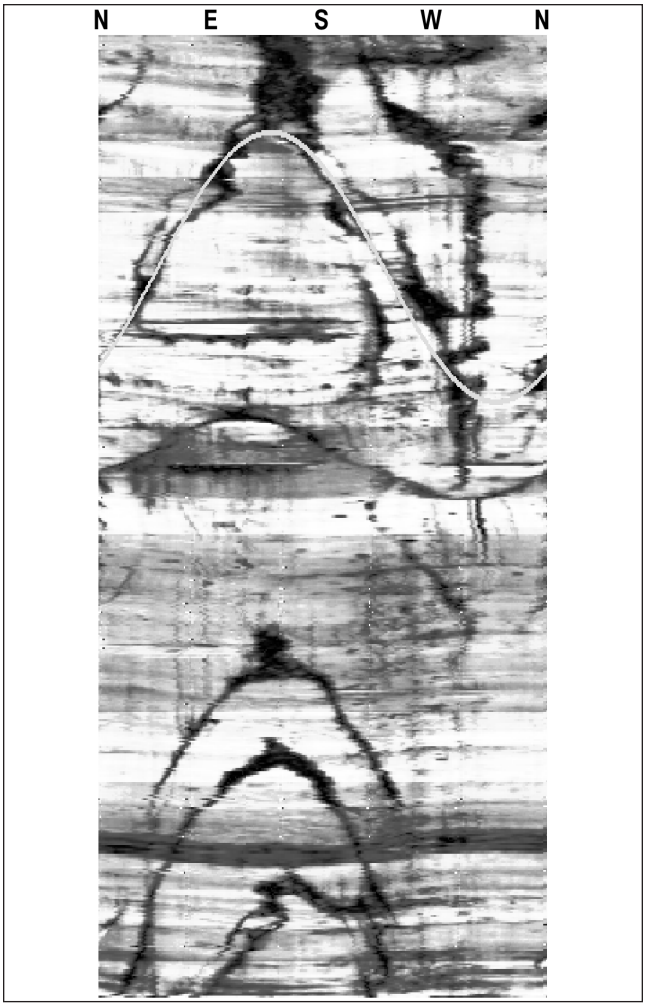

Figure 2. Standard 2-D "unwrapped" view of acoustic-image data. The vertical axis is depth; the horizontal axis is azimuth around the wellbore. Where fractures are intersected by the borehole, rock is weakened selectively and eroded. Erosion is concentrated at featheredges of fractures, chiefly at the "peaks" and "troughs" of sinusoids that are formed by traces of fractures on the wall of the borehole. Gradation of black, gray, and white shows variation in amplitude of the acoustic signal—the higher the amplitude, the lighter the color. Observe that sinusoids are shown in dark patterns and that the curves tend to be broader and darker at "peaks" and "troughs," where the most rock has broken from the borehole wall.

IMPLICATIONS FOR FRACTURED RESERVOIRS

In most fractured reservoirs, the natural fractures and faults are the primary pathways for fluid flow. We have used comprehensive information about in-situ stress, fracture, and flow from several fractured reservoirs and have found that

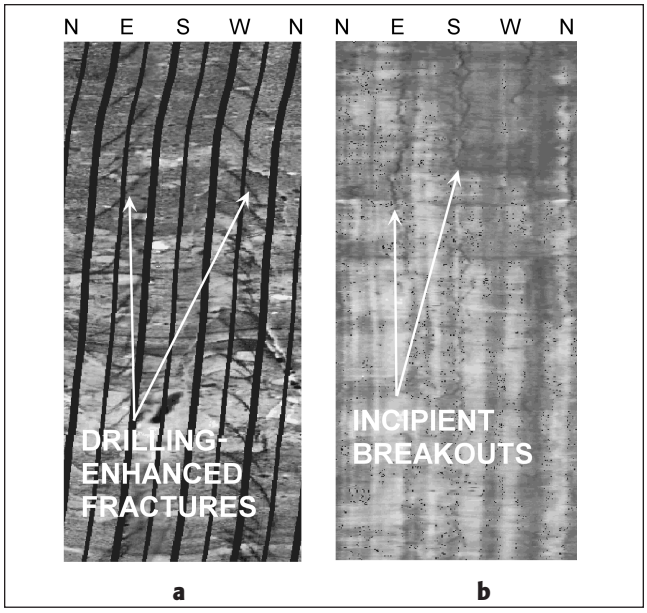

Figure 3. Electrical-image data showing (a) drilling-enhanced fractures in a vertical borehole and (b) incipient wellbore breakouts detected in acoustic-image data.

critically stressed faults (in a reservoir, the subset of preexisting faults that is active in today's stress field) systematically control permeability (Barton et al., 1995). Thus, although we agree with the many scientists who have suggested that the state of stress may influence transmissivity of fractures, the critically stressed faults are the most permeable fractures in situ—not Mode I tensile fractures, as is generally thought. We demonstrate how this new, predictable relationship between in-situ stress and permeability can be used to optimize production from fractured and faulted petroleum and geothermal reservoirs.

FRACTURE AND FLUID-FLOW ANALYSIS

Precision temperature logs and/or spinner flowmeter logs provide information on the hydraulic conductivity of individual fractures and faults. Fluid flow into or out of individual fractures and faults can be determined through analyses of these logs (Paillet and Ollila, 1994). Where a borehole is close to thermal equilibrium with surrounding rock, heat transfer primarily is by thermal conduction, and the temperature gradient in the borehole is a function of thermal conductivity and heat flux. Localized perturbations of wellbore temperature result from localized fluid flow in the borehole; they can be detected by precision temperature logging. Therefore, fractures or faults that correlate in depth with these localized temperature perturbations are considered to be hydraulically conductive. Multipass temperature logs at various rates of pumping allow assessment of the persistence of these horizons of flow. Figure 5 shows wellbore-image data correlated with a temperature gradient log of a well in the producing reservoir at Dixie Valley, Nevada.

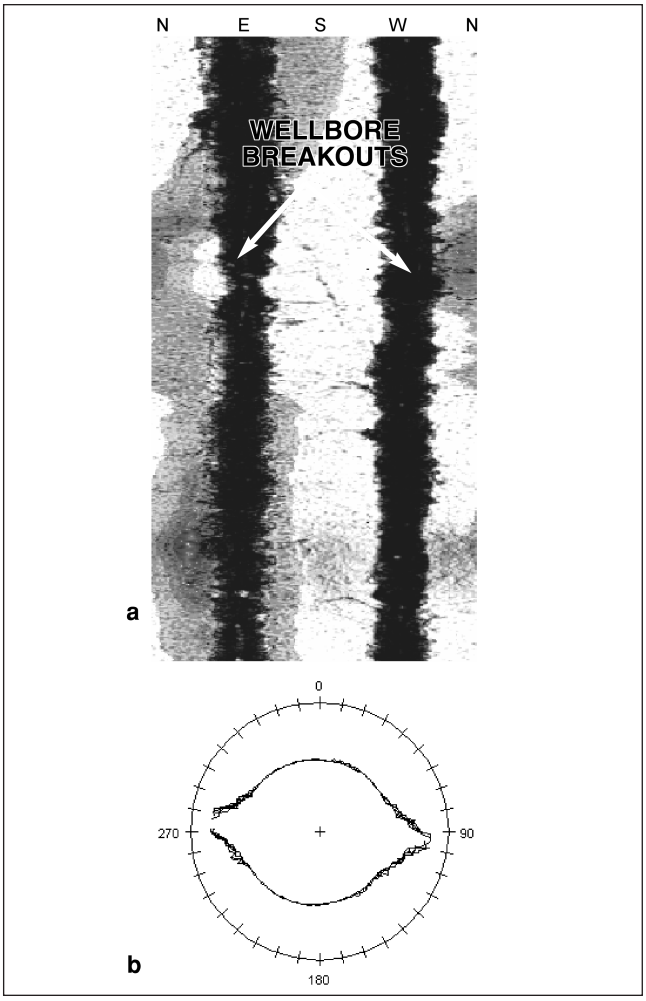

Figure 4. (a) Unwrapped view of well-developed breakouts in acoustic-image data. (b) Polar cross section of breakouts in a different well, used to accurately measure breakout azimuth (in this case, 20° to 25° and 210° to 250°) and width (indicated by light gray lines).

COULOMB FAILURE ANALYSIS

By using results from in-situ stress measurements and evidence of wellbore failure in wellbore-image data, proximity of fractures and faults to Coulomb (i.e., frictional) failure can be determined. To apply the Coulomb criterion to a population of fractures, orientations and magnitudes of the three in-situ principal stresses and formation-fluid pressure must be known.

Shear stress and effective normal stress (i.e., S_n–P_p) acting on each fracture plane are then functions of (a) the principal stress magnitudes, (b) fluid pressure, and (c) orientation of the fracture plane with respect to orientations of the principal stresses (Jaeger and Cook, 1979).

Results of a Coulomb failure analysis are depicted as 3-D Mohr diagrams of shear versus effective normal stress (see Figure 6 and refer to Jaeger and Cook, 1979, for explanation of the construction of these diagrams). Fractures that lie above the Coulomb failure line for $\mu = 0.6$ are critically stressed, potentially active faults in frictional equilibrium with the current in-situ stress field. Based on laboratory measurement of the frictional strength of prefractured rock (Byerlee, 1978), we assume that fractures with a ratio of shear-to-normal stress ≈ 0.6 are oriented to the stress field optimally for frictional failure. Fractures that lie below the $\mu = 0.6$ Coulomb failure curve are not critically stressed shear fractures. The ratio of shear to normal stress on these fractures is insufficient to promote slip.

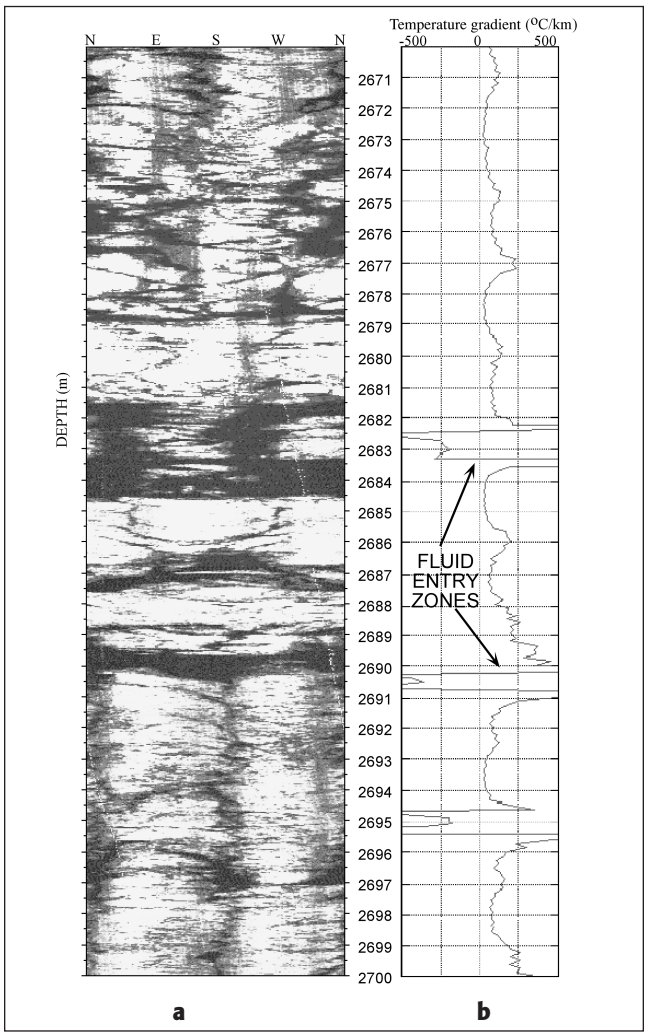

Figure 5. (a) Unwrapped view, acoustic high-temperature borehole-televiewer data recorded over the interval 2670–2700 m in well 37-33. The interval is in the producing reservoir at Dixie Valley and is correlated with temperature-gradient data recorded over the same interval. (b) Extremely large anomalies in the temperature gradient (for example, 2682.5, 2690.5, and 2695) are at the depth locations of fractures and faults where high-temperature fluids enter the borehole.

DEEP-RESERVOIR PERMEABILITY: TWO EXAMPLES

The Dixie Valley geothermal field, a fault-controlled geothermal reservoir in the Basin and Range Province of the western United States, has been the focus of a thorough study of the relationship between in-situ stress and fracture permeability. The Stillwater fault, an active range-bounding normal fault, is the producing reservoir for a geothermal plant operated by Oxbow Geothermal Corporation. However, well-documented lateral variations in productivity along the fault are not fully understood. An ongoing, integrated study of the fractured-rock hydrology within and outside the producing reservoir at Dixie Valley demonstrates the relationship between crustal fluid flow and the contemporary in-situ stress

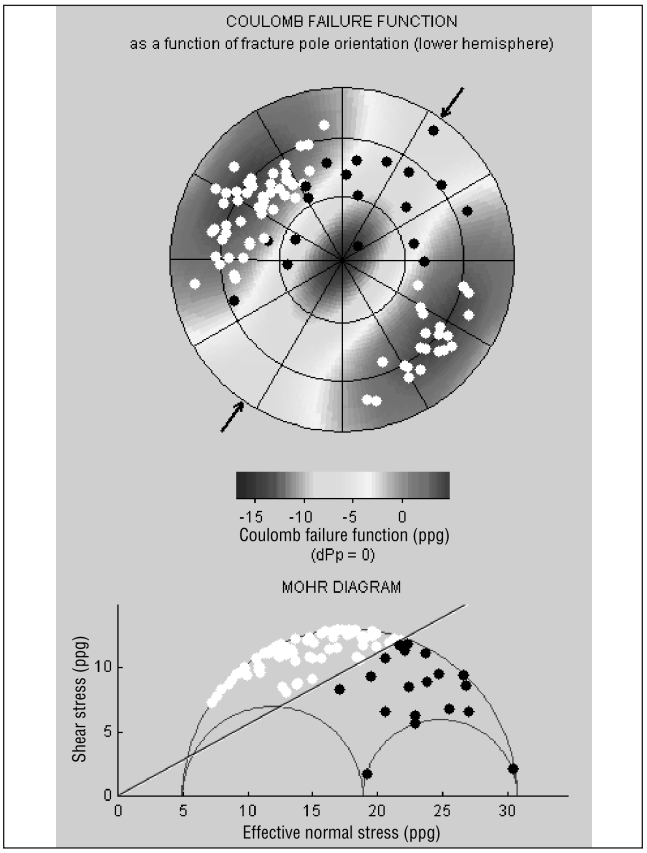

Figure 6. The upper plot shows lower-hemisphere stereographic projection of poles to hydraulically conductive fracture planes in Dixie Valley well 73B-7. White symbols represent poles of fractures that are optimally oriented and critically stressed for frictional failure. The lower plot is a 3-D Mohr diagram including the Coulomb frictional-failure line. White symbols represent critically stressed fracture planes. Note that the points representing most hydraulically conductive fractures are above the Coulomb failure line and that the fractures can maintain permeability through repeated stress-induced slip. In this figure, ppg is pounds per gallon and dPp is the difference between borehole fluid pressure and formation pore pressure.

field in this producing geothermal reservoir (Barton et al., 1998; Hickman and Zoback, 1998).

Sets of borehole televiewer (BHTV) logs, precision temperature logs, and spinner flowmeter (TPS) logs were recorded from wells in the primary area of geothermal production (transmissivities on the order of 1 m^2/min) and from wells in a few kilometers of the producing area. In this latter set of wells, rock is relatively impermeable; hence, the wells are not commercially viable (transmissivities of about 10^{-4} m^2/min). From these logs, natural fractures and faults were measured and their hydrologic properties studied by comparison with fracture-related thermal and flow anomalies. Observations of wellbore failure (breakouts and cooling cracks)—together with hydraulic-fracturing stress measurements made in these wells—provided complete data for a systematic, comparative study of the effects of in-situ stress on fracture permeability along productive and nonproductive segments of the fault. Fractures or faults that correlate in depth with localized perturbations of temperature are considered to be hydraulically conductive.

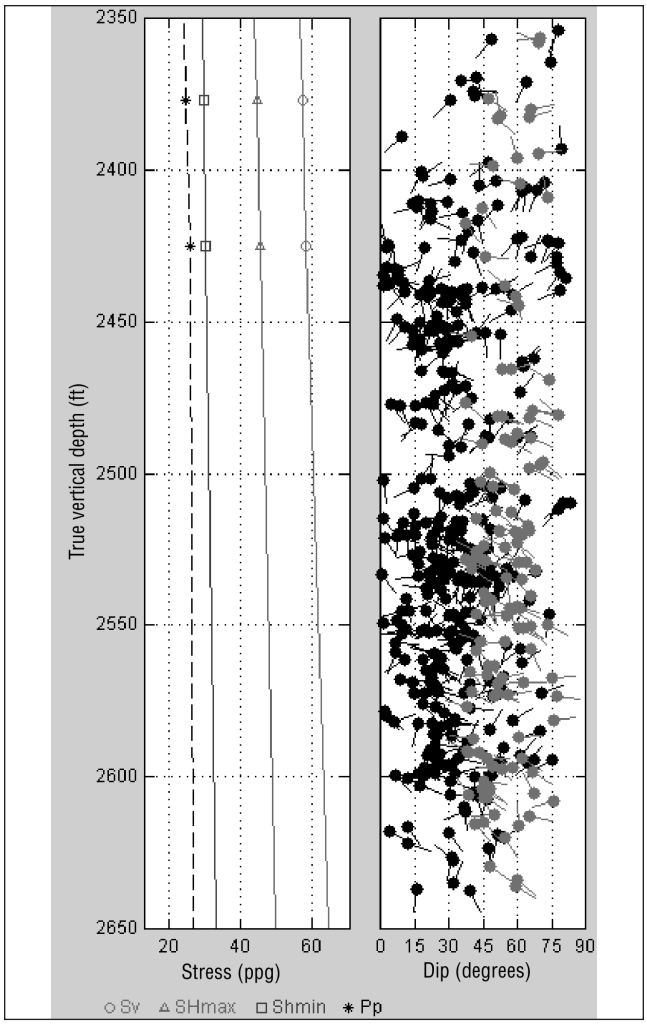

Figure 7. Principal-stress magnitudes (left plot; after Hickman and Zoback, 1998) and natural fracture population (right plot) measured in well 73B-7 at the Dixie Valley geothermal field in Nevada. S_v is vertical stress; S_{Hmax} is maximum horizontal principal stress; S_{hmin} is the least horizontal principal stress; P_p is the pore pressure. The fracture tadpoles shown in gray define the subset of optimally oriented and critically stressed fractures in this well.

The analysis of fractures and fluid flow indicates that in producing and nonproducing wells alike, relatively few fractures dominate flow. The populations of highly permeable fractures in wells that penetrate the producing segment of the Stillwater fault (for example, well 73B-7, gray tadpoles in Figure 7) clearly define a distinct subset of the total fracture population in each well. This subset is normal to the local direction of the least principal stress in the horizontal plane, S_{hmin}.

Stress orientations and magnitudes measured in these wells, fracture orientations obtained from BHTV logs, and measured formation-fluid pressures were used to calculate the shear and normal stress on each of the fracture planes. The Coulomb failure criterion was the means to determine whether each plane was a potentially active fault. For the example well 73B-7, this analysis was performed for fractures characterized as hydraulically conductive, based on spinner flowmeter logs and temperature gradient logs. For each 1-m depth interval in which no temperature or spinner anomaly was detected, the dominant fracture trend was selected as a control group of fractures that were not hydraulically conductive.

Results of the analysis indicate that fracture zones with high measured permeabilities and within the producing segment of the fault are parallel to the local trend of the Stillwater fault. Also, they are optimally oriented and critically stressed for frictional failure in the overall east-southeast extensional stress regime measured at the site. Figure 6 presents a typical example of the hydraulically conductive fractures identified from well 73B-7. The top part of Figure 6 is a stereographic projection of poles to the permeable fracture planes. Gray-scale coloring in this plot represents the proximity of these planes to frictional failure. White symbols denote planes that are critically stressed shear planes. The lower plot in this figure shows the same fracture distribution in 3-D Mohr representation. White symbols show the critically stressed fractures and black symbols show stable planes. Although the data are scattered, most permeable fractures plot above or near the $\mu = 0.6$ Coulomb failure line. Results similar to these presented for well 73B-7 were obtained from analysis of each commercially productive well of the Dixie Valley field.

In contrast, most nonconductive fractures identified in well 73B-7 plot below the Coulomb failure curve and therefore do not appear to be critically stressed shear fractures

(Figure 8). Nonproducing wells south of producing wells at Dixie Valley were found to have (1) available shear stress insufficient to drive fault slip or (2) fracture and fault populations misoriented for normal faulting in the current stress field. In Dixie Valley, fault-zone permeability is high only where individual fractures as well as the overall Stillwater fault zone are optimally oriented and critically stressed for frictional failure.

In a second example, stress-induced wellbore breakouts and tensile wall fractures were analyzed in wellbore-image data recorded in wells drilled into a producing petroleum reservoir in the western United States. These wellbore failures were used to determine the full stress tensor throughout the field. The natural fracture population of this sandstone-and-shale reservoir also was characterized through wellbore-image analysis. The primary purpose of the analyses was to determine the optimal drilling trajectories, which would expose boreholes in this field to the greatest population of oil-filled fractures.

Determining the set of critically stressed fractures in the reservoir by Coulomb failure analysis is straightforward when stress orientations and magnitudes are constrained. Figure 9 shows results of this technique applied to one of the wells of this field, which demonstrates the importance of the relationship between the state of stress and fracture permeability. Although two significant clusters of natural fractures are in this example, only one fracture set is optimally oriented to the stress field. These fractures are strong hydraulic conductors because the crust is in frictional equilibrium and therefore conducive to repeated stress-induced slip.

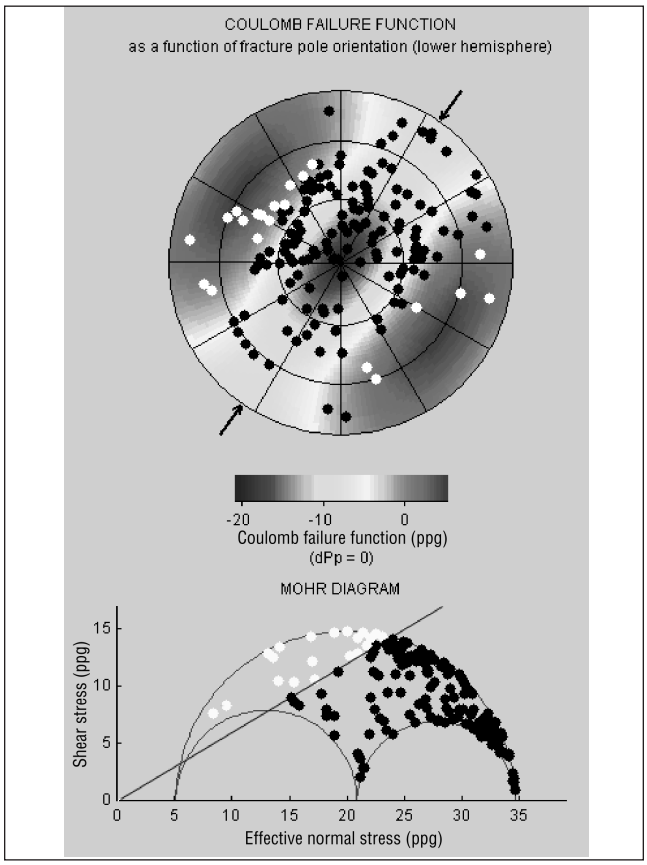

Figure 8. The upper plot shows lower-hemisphere stereographic projection of poles to nonhydraulically conductive fracture planes in Dixie Valley well 73B-7. White symbols represent poles of fractures that are optimally oriented and critically stressed for frictional failure. The lower plot is a 3-D Mohr diagram including the Coulomb frictional-failure line. White symbols represent critically stressed fracture planes. Note that the points representing most nonhydraulically conductive fractures are near or below the Coulomb failure line and that the fractures, therefore, are stable planes. In this figure, ppg is pounds per gallon and dPp is the difference between borehole fluid pressure and formation pore pressure.

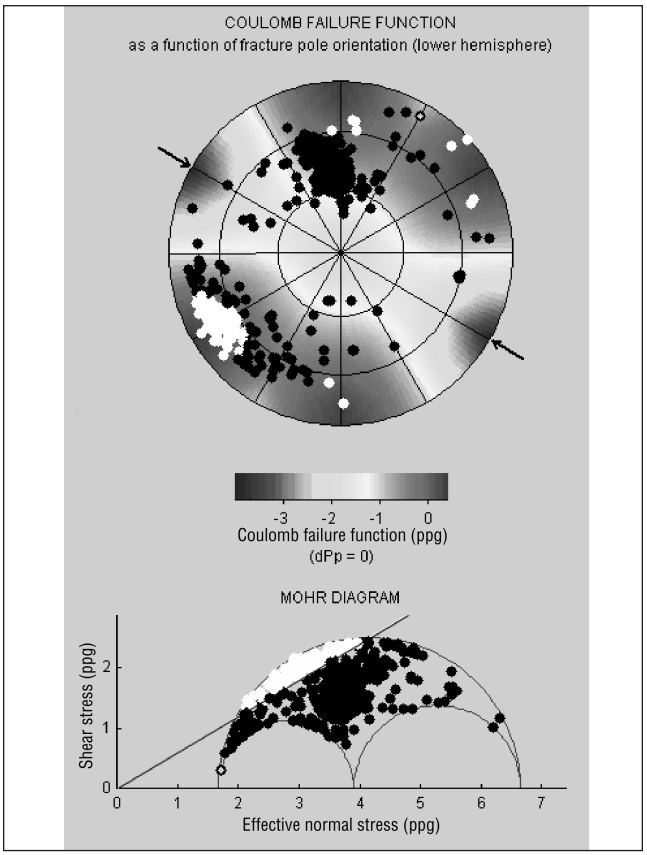

Figure 9. The upper plot shows lower-hemisphere stereographic projection of poles to all fracture planes in a well in an oil field in the western United States. White symbols represent poles of fractures that are optimally oriented and critically stressed for frictional failure. The lower plot is a 3-D Mohr diagram including the Coulomb frictional-failure line. White symbols represent critically stressed fracture planes. Note that the optimal trajectory for drilling a well perpendicular to the greatest population of critically stressed fractures is to the southwest. In this figure, ppg is pounds per gallon and dPp is the difference between borehole fluid pressure and formation pore pressure.

To exploit the maximal number of critically stressed fractures in this portion of the field, the optimal borehole trajectory should be southwestward, with inclination of about 70°. In the stereographic projection in Figure 9, this would correspond to a trajectory drilled in the direction of the cluster of white symbols. In support of this analysis, steeply inclined wells drilled to southwestward in this field do produce petroleum in relatively large volumes. Production from wells drilled in other directions in this field is poor to nonexistent.

SHALLOW RESERVOIR PERMEABILITY: THE ADCOH CASE STUDY

In regions where competent basement rock is close to the surface, in-situ stress measurements can be made in a straightforward manner. Where shallow bedrock is the target, lithology of a site investigation is precisely where fluid flow is expected to be fracture controlled. The southeastern United States provides an excellent example of such a case. In 1985, near the border of North Carolina and Georgia, wellbore-image logs, hydraulic-fracturing logs, and precision-temperature logs were recorded in wells shallower than 300 m, as part of the Appalachian Deep Corehole site investigation. Well ADCOH No. 2 was drilled into gneissic and phyllitic rocks of the Brevard Fault Zone; ADCOH No. 4 penetrated schists and gneisses of the Blue Ridge.

Hydraulic-fracturing stress measurements were made at multiple depths in these wells. They indicate a reverse-faulting state of stress, consistent with the regional Appalachian compressional tectonics. In well ADCOH No. 2, values of the least horizontal principal stress, S_{hmin}, are close to the vertical stress, which indicates that the state of stress is more reverse/strike-slip than in well No. 4. The latter well, drilled in the Blue Ridge, shows a pure reverse-faulting state of stress (Figure 10). Prehydrofrac and posthydrofrac borehole-televiewer logging reveals that the orientation of induced hydraulic fractures is northeast-southwest, consistent with other in-situ stress measurements made in the shallow crust and at depth in the southeastern United States (Moos and Zoback, 1993).

Depth distributions and relative apertures of natural fractures were measured from borehole-televiewer data recorded in the study wells. The measured fracture population of well ADCOH No. 2 is predominantly high-angle, oriented in the direction of maximum horizontal principal stress (Figure 11, left plot). These fracture sets probably are related to development of extensional basins along the eastern margin of North America during the Triassic Period. Well ADCOH No. 4 also has a well-developed high-angle fracture population, in addition to a distinct population of a shallower east-dipping set of fractures (Figure 11, right plot).

Precision-temperature data were recorded in each of the site-investigation wells (J. Costain, personal communication, 1999). Gradients computed from temperature logs recorded in each well show significant variation with depth, indicating fluid flow at the borehole wall along relatively permeable fractures and faults. Depths of significant temperature anomalies were used to determine the population of hydraulically conductive fractures in each fracture set (light gray symbols, Figure 11).

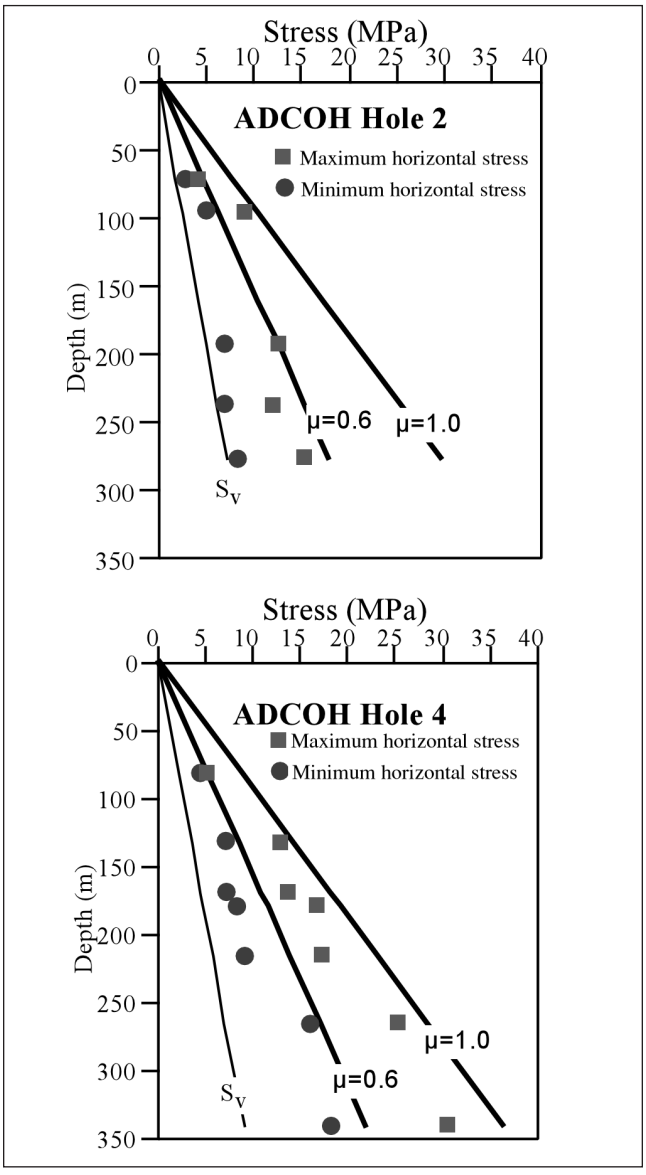

Figure 10. Hydraulic-fracturing stress measurements made in wells No. 2 and No. 4 of the ADCOH study site. The measurements indicate a reverse-faulting state of stress in the shallow crust. Stress scaled in megapascals. S_v signifies vertical stress.

The hydraulically conductive fractures in well ADCOH No. 2 are high-angle faults, as is the predominant fracture population, and they cannot be distinguished readily from the overall fracture orientation (Figure 11, left plot). However, hydraulically conductive fractures in well ADCOH No. 4 form a distinct subset in the overall fracture population, correlating with the moderate to shallow east-dipping fracture set (Figure 11, right plot, black symbols).

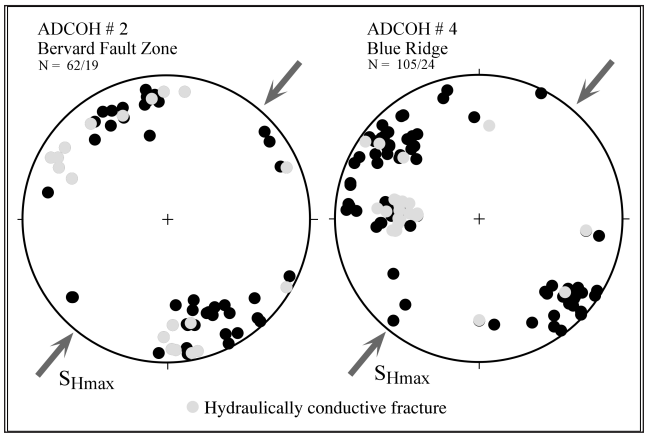

Figure 11. Poles to measured fracture planes for wells No. 2 and No. 4 of the ADCOH study site. Poles of fractures that depth-correlate with temperature-gradient anomalies are shown in light gray. Numbers of samples: Numerator shows total number of poles plotted; denominator shows number of fractures correlated with temperature-gradient anomalies.

Coulomb failure analysis of fracture populations from these shallow wells clearly shows that hydraulically conductive fractures are critically stressed and optimally oriented for frictional failure in the measured stress field of these wells (Figure 12a). The Mohr analysis of well ADCOH No. 2 indicates that many fractures are optimally oriented but few are critically stressed in the measured stress field.

Where there are two distinct fracture populations in well ADCOH No. 4, the subset of hydraulically conductive fractures is optimally oriented for reverse faulting in the present-day stress field (Figure 12b). Higher-angle fractures that correlate with fluid-flow anomalies probably are ancient normal faults, reactivated in a reverse sense of slip.

SUMMARY

Wellbore-image interpretation is an important aspect of geomechanical modeling. Discrimination between drilling-induced and natural phenomena in borehole data is guided best by use of a set of specialized image-analysis tools and an understanding of wellbore geomechanics. Misinterpretation of wellbore images can lead to significant error in geomechanical modeling, and hence to inappropriate analyses of reservoir permeability and wellbore stability.

The performance of low-permeability, fractured, and often overpressured reservoirs is controlled by the in-situ

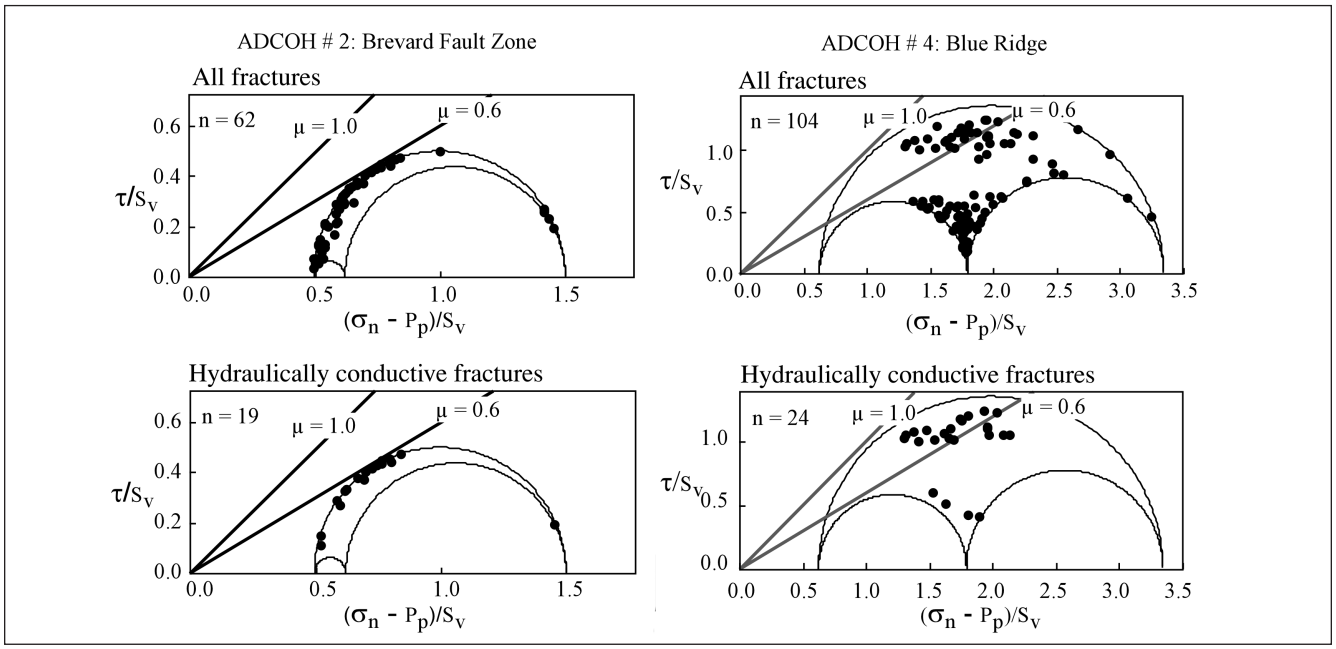

a b

Figure 12. (a) Normalized shear versus effective normal stress for all measured fractures in well ADCOH No. 2 (top) and for hydraulically conductive fractures (bottom) of the ADCOH study site. (b) Normalized shear versus effective normal stress for all measured fractures in well ADCOH No. 4 (top) and for hydraulically conductive fractures (bottom) of the ADCOH study site. Axes are labeled as follows: $(\sigma_n\text{-}P_p)/S_v$ shows ratio of (normal stress-pore pressure) normalized relative to vertical stress, whereas τ/S_v shows shear stress normalized relative to vertical stress.

state of stress and by the distribution and orientation of natural fractures and faults. Of the total number of fractures, only a subset is likely to be permeable, and the orientation of this subset is controlled by the state of stress. Maximizing production from a fractured reservoir requires placement of wells in this manner: Under constraints of well spacing, each borehole is directed so as to intersect the greatest number of permeable fractures.

In a variety of wells drilled to midcrustal depths, the high degree of correlation between critically stressed faults and hydraulic conductivity appears to hold, regardless of the type of reservoir fluid or the lithology of the reservoir. This correlation appears to hold in rocks near the surface, providing a new means of characterizing the hydrology of the shallow crust.

ACKNOWLEDGMENTS

The Dixie Valley study is supported by the U. S. Department of Energy (DOE) Geothermal Technologies Program. However, any opinions, findings, conclusions, or recommendations expressed herein are those of the authors and do not necessarily reflect the views of the DOE. Support for the ADCOH study was supplied by the National Science Foundation, the Stanford University Department of Geophysics, and GeoMechanics International, Inc.

REFERENCES CITED

Aadnoy, B. S., 1990, In-situ stress direction from borehole fracture traces: Journal of Petroleum Science Engineering, v. 4, p. 143–153.

Barton, C. A., and M. D. Zoback, 1992, Self-similar distribution and properties of macroscopic fractures at depth in crystalline rock in the Cajon Pass scientific drillhole: Journal of Geophysical Research, v. 97, no. B4, p. 5181–5200.

Barton, C. A., M. D. Zoback, and K. L. Burns, 1988, In-situ stress orientation and magnitude at the Fenton geothermal site, New Mexico, determined from wellbore breakouts: Geophysical Research Letters, v. 15, p. 467–470.

Barton, C. A., M. D. Zoback, and D. Moos, 1995, Fluid flow along potentially active faults in crystalline rock: Geology, v. 23, no. 8, p. 683–686.

Barton, C. A., D. Moos, P. Peska, and M. D. Zoback, 1997, Utilizing wellbore image data to determine the complete stress tensor: Application to permeability anisotropy and wellbore stability: The Log Analyst, v. 38, no. 6, p. 21–33.

Barton, C. A., S. Hickman, R. Morin, M. D. Zoback, and D. Benoit, 1998, Reservoir-scale fracture permeability in the Dixie Valley, Nevada, geothermal field: Society of Petroleum Engineers/International Society of Rock Mechanics, paper 47371, *in* Proceedings of Eurock '98, Rock Mechanics in Petroleum Engineering, July, Trondheim, Norway, p. 1–8.

Brudy, M., and M. D. Zoback, 1993, Compressive and tensile failure of boreholes arbitrarily-inclined to principal stress axis: Application to the KTB boreholes, Germany: 34th U.S. Rock Mechanics Symposium, International Journal of Rock Mechanics, Mineral Science and Geomechanical Abstracts, v. 30, no. 7, p. 1035–1038.

Brudy, M., and M. D. Zoback, 1999, Drilling-induced tensile wall fractures: Implications for determination of in-situ stress orientation and magnitude: International Journal of Rock Mechanics, Mineral Science and Geomechanical Abstracts, v. 36, no. 2, p. 191–215.

Brudy, M., and H. Kjorholt, 1999, The initiation of drilling-induced tensile fractures and their use for the estimation of stress magnitude, *in* Amadei, Kranz, Scott, and Smeallie, eds., Rock mechanics for industry: Rotterdam, Balkema, p. 1189–1194.

Byerlee, J., 1978, Friction of rocks: Pure and Applied Geophysics, v. 116, p. 615–626.

Castillo, D. A., and D. Moos, 2000, Reservoir geomechanics applied to drilling and completion programs in challenging formations: Northwest Shelf, Timor Sea, North Sea and Colombia: Australian Petroleum Production and Exploration Association Journal, p. 509–521.

Finkbeiner, T., C. A. Barton, and M. D. Zoback, 1997, Relationship between in-situ stress, fractures and faults, and fluid flow in the Monterey Formation, Santa Maria Basin, California: AAPG Bulletin, v. 81, no. 12, p. 1975–1999.

Gough, D. I., and J. S. Bell, 1981, Stress orientations from borehole wall fractures with examples from Colorado, east Texas, and northern Canada: Canadian Journal of Earth Sciences, v. 19, p. 1358–1370.

Hayashi, K., and H. Abe, 1984, A new method for the measurement of in situ stress in geothermal fields: Journal of Geothermal Research Society of Japan, v. 6, p. 203–212.

Hickman, S., and M. D. Zoback, 1998, Tectonic controls on fracture permeability in a geothermal reservoir at Dixie Valley, Nevada: Society of Petroleum Engineers/International Society of Rock Mechanics, paper 47213, *in* Proceedings of Eurock '98, Rock Mechanics in Petroleum Engineering, July, Trondheim, Norway, p. 1–8.

Hubbert, M. K., and D. G. Willis, 1957, Mechanics of hydraulic fracturing: American Institute of Mining, Metallurgical, and Petroleum Engineers Transactions, v. 210, p. 153–168.

Jaeger, J. C., and N. G. W. Cook, 1979, Fundamentals of rock mechanics, 3rd ed.: New York, Chapman and Hall, p. 28–30.

Moos, D., and M. D. Zoback, 1990, Utilization of observations related to wellbore failure to constrain the orientation and magnitude of crustal stresses: Application to continental, DSDP and ODP boreholes: Journal of Geophysical Research, v. 95, p. 9305–9325.

Moos, D., and M. D. Zoback, 1993, Near-surface, "thin skin" reverse-faulting stresses in the southeastern United States: 34th U.S. Symposium on Rock Mechanics, International Journal of Rock Mechanics, Mineral Science and Geomechanical Abstracts, v. 30, no. 7, p. 965–971.

Okabe, T., N. Shinohara, and S. Takasugi, 1996, Earth's crust stress field estimation by using vertical fractures caused by borehole drilling: Proceedings of the 8th International Symposium on the Observation of the Continental Crust through Drilling, Tsukuba, Japan, February 26–28, p. 265–270.

Paillet, F. L., and P. Ollila, 1994, Identification, characterization, and analysis of hydraulically conductive fractures in granitic basement rocks, Millville, Massachusetts: U. S. Geological Survey Water Resources Investigations, paper 94–4185.

Peska, P., and M. D. Zoback, 1995, Compressive and tensile failure of inclined wellbores and determination of in situ stress and rock strength: Journal of Geophysical Research, v. 100, no. B7, p. 12791–12811.

Plumb, R. A., and S. H. Hickman, 1985, Stress-induced borehole elongation—a comparison between the four-arm dipmeter and the borehole televiewer in the Auburn geothermal well: Journal of Geophysical Research, v. 90, no. B7, p. 5513–5521.

Rezmer-Cooper, I., T. Bratton, and H. Krabbe, 2000, The use of resistivity-at-the-bit images and annular pressure while drilling in preventing drilling problems: International Association of Drilling Contractors/Society of Petroleum Engineers, paper 59225, 2000 IADC/SPE Drilling Conference, New Orleans, February 23–25, p. 1–13.

Shamir, G., and M. D. Zoback, 1992, Stress orientation profile to 3.5 km depth near the San Andreas fault at Cajon Pass, California: Journal of Geophysical Research, v. 97, p. 5059–5080.

Stjern, G., P. Horsrud, and A. Agle, 2000, Improving drilling performance in troublesome clay formations in the Heidrun field: International Association of Drilling Contractors/Society of Petroleum Engineers, paper 59219, 2000 IADC/SPE Drilling Conference, New Orleans, February 23–25, p. 1–10.

Willson, S., N. C. Last, M. D. Zoback, and D. Moos, 1999, Drilling in South America: A wellbore stability approach for complex geologic conditions: Society of Petroleum Engineers, paper 53940, p. 1–10, *in* 1999 Society of Petroleum Engineers, Latin American and Caribbean Petroleum Engineering Conference, Caracas, Venezuela, April 21–23.

Wiprut, D., and M. D. Zoback, 2000, Constraining the full stress tensor in the Visund field, Norwegian North Sea: Application to wellbore stability and sand production: International Journal of Rock Mechanics, February 2000, v. 37, nos. 1–2, p. 317–336.

Zoback, M. D., and P. Peska, 1995, In-situ stress and rock strength in the GBRN/DOE Pathfinder well, South Eugene Island, Gulf of Mexico: Journal of Petroleum Technology, v. 47, no. 5, p. 582–585.

Zoback, M. D., D. Moos, L. Mastin, and R. N. Anderson, 1985, Wellbore breakouts and in-situ stress: Journal of Geophysical Research, v. 90, p. 5523–5530.